

Anomalous Slowdown of Polymer Detachment Dynamics on Carbon Nanotubes

Daniel A. Vega,^{1,*} Andrey Milchev,^{2,†} Friederike Schmid,^{2,1} and Mariano Febbo¹

¹*Instituto de Física del Sur (IFISUR) and Departamento de Física, Universidad Nacional del Sur (UNS), Consejo Nacional de Investigaciones Científicas y Técnicas—CONICET, Avenida L. N. Alem 1253, 8000 Bahía Blanca, Argentina*

²*Institute of Physics, Johannes Gutenberg University Mainz, Staudingerweg 7, 55128 Mainz, Germany*

 (Received 10 March 2019; published 31 May 2019)

The “wrapping” of polymer chains on the surface of carbon nanotubes allows one to obtain multifunctional hybrid materials with unique properties for a wide range of applications in biomedicine, electronics, nanocomposites, biosensors, and solar cell technologies. We study by means of molecular dynamics simulations the force-assisted desorption kinetics of a polymer from the surface of a carbon nanotube. We find that, due to the geometric coupling between the adsorbing surface and the conformation of the macromolecule, the process of desorption slows down dramatically upon increasing the windings around the nanotube. This behavior can be rationalized in terms of an overdamped dynamics with a frictional force that increases exponentially with the number of windings of the macromolecule, resembling the Euler-Eytelwein mechanism that describes the interplay between applied tension and frictional forces on a rope wrapped around a curved surface. The results highlight the fundamental role played by the geometry to control the dynamics and mechanical stability of hybrid materials in order to tailor properties and maximize performance.

DOI: [10.1103/PhysRevLett.122.218003](https://doi.org/10.1103/PhysRevLett.122.218003)

From ancient times up to now, the interplay of the frictional forces and the tension on a rope wrapped around a solid support or another rope has been employed in a myriad of applications. Indeed, the first use of ropes for hunting, pulling, lifting, climbing, fastening, etc., is believed to date back to prehistoric times and predates the use of the axe (6000 B.C.) or the wheel (5000 B.C.), and probably even the controlled use of fire (125 000 B.C.) [1]. Winding a rope around a curved surface not only allows one to transmit an applied force along a different direction but also to strongly reduce the tension from one end to the other. This feature was exploited in Leonardo da Vinci’s machines and in tools dating back as far as ancient Egypt, and it is also employed in nature by tendril-producing plants [2,3], like grape or passionflowers, and it is exploited by different mammals with prehensile tails, like the harvest mouse or New World monkeys, to hold on to branches (see Fig. 1), climb trees, and grab or manipulate objects [4].

Geometrical properties are also relevant on the nanoscale, for example when considering the interactions between macromolecules and carbon nanotubes. “Wrapping” polymer chains around the surface of single wall carbon nanotubes (SWCNTs) allows one to control their solubility in different solvents and also to create novel materials for materials science [5–10], medicine [11–13], biosensor technology [14], DNA sequencing [15,16], and nanoelectronics [17]. For example, short sequences of single-stranded DNA can be employed to sort SWCNTs by diameter, chirality, or electronic behavior, and hybrid

nanomaterials combining biopolymers with SWCNTs have recently been utilized in a variety of applications such as drug delivery, imaging, and sensing [18–20]. Using hybrid materials in applications requires a solid knowledge of the

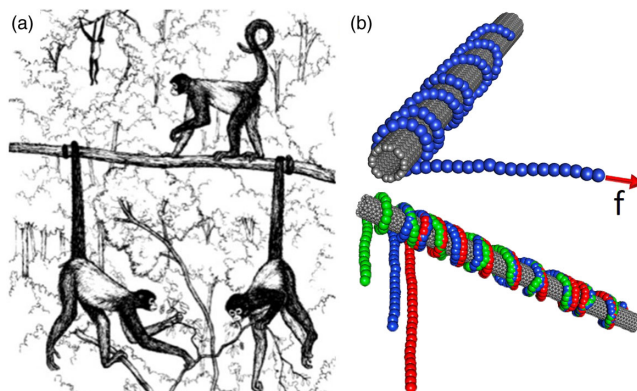


FIG. 1. Interplay between tension and friction on the macro- and nanoscale. (a) Black spider monkeys (*Ateles paniscus*) can use their prehensile tails to hold onto branches. The friction between the prehensile tail and the surface of the branch is strongly enhanced due to its helical wrapping around the branch (adapted from Ref. [4]). (b) Macromolecule adsorbed on a nanotube partially detached by the presence of an external force \mathbf{f} acting on one of the chain ends. Here we consider external forces that point along the direction perpendicular to the tube axis. The lower panel shows the polymer configuration at three different desorption times.

stability of the assembly depending on the conformation, the molecular size, and the binding energy [18–21].

For example, the thermal stability of DNA-SWCNT hybrids was found to increase sharply with increasing DNA sequence length [22]. Depending on the architecture of the molecule, the self-organized structures and winding of the molecule around the tube can be controlled. For example, polysaccharide chains like chitosan [23] or phenylene-ethylene [24] polymers adopt a helical conformation when adhered to SWNTs, while DNA makes a complete right-handed helical wrap around the SWCNT [18].

As a first step towards understanding the leading factors that control the mechanisms of desorption of a polymer chain from a carbon nanotube, here we use molecular dynamics (MD) simulations of a coarse-grained model to study the role of the geometry of the adsorbing surface on the dynamics of force-assisted polymer detachment [see Fig. 1(b)]. Our central finding can be summarized as follows: We demonstrate the existence of a geometrically controlled friction phenomenon that drastically slows down the desorption process. We analyze this effect quantitatively and show that it is closely related to the capstan mechanism—a well-known macroscopic phenomenon that is relevant for many human activities. Hence we show that the same mechanism may also control the interactions of hybrid materials at the nanoscale and thus unveil universal aspects of the phenomenon.

To investigate the mechanisms of force-assisted desorption, we consider polymers with different conformations that are adsorbed on the surface of a SWCNT with a honeycomb structure in the armchair configuration. In order to investigate the geometric effect of the nanotube curvature, we choose a system with a relatively small tube diameter (0.55 nm, considering the bond length of carbon atoms as 1.44 Å) [17,25]. The good solvent condition is implicitly implemented by using purely repulsive nonbonded interactions of the Weeks-Chandler-Andersen (WCA) type: $U^{\text{WCA}}(r) = 4\epsilon[(\sigma/r)^{12} - (\sigma/r)^6 + \frac{1}{4}]$, $r \leq b$, and $U^{\text{WCA}}(r > b) = 0$. Here ϵ and σ are the units of energy and length, respectively. The parameter σ fixes the bond length at equilibrium ($b = 2^{1/6}\sigma \approx 1.12$), and ϵ is expressed in units of $k_B T$, where k_B is the Boltzmann constant, and T is the temperature [26]. The “MD units” of our Letter are given in terms of σ and $k_B T$. In our MD simulations, we use a coarse-grained model of a polymer chain of N beads connected by finitely extendable elastic bonds [27] [see Fig. 1(b)]. The bonded interaction between the neighbor monomers along the polymer chain is described by the finitely extensible nonlinear elastic (FENE) potential, $U_{\text{FENE}}(r) = -\frac{1}{2}kr_0^2 \ln[1 - (r^2/r_0^2)]$, $r \leq r_0$, and $U_{\text{FENE}}(r > r_0) = \infty$, with $k = 30\epsilon/\sigma^2$ and $r_0 = 1.5\sigma$. The chain stiffness is controlled by the bending potential: $U_{\text{bend}}(\theta) = \kappa(1 - \cos\beta)$, where β is the bond angle formed between two subsequent bond vectors. The bending stiffness is controlled through the parameter κ . The

attractive interaction of the chain beads with the tube is given by the conventional Lennard-Jones potential with a cutoff of 2.5σ in the MD code. Here we use the model parameters $\kappa = 15k_B T$ with $k_B T = 1$.

The time evolution of polymer desorption is calculated by solving a Langevin equation of motion for the position \mathbf{r}_i of each bead along the chain: $m\dot{\mathbf{r}}_i = \mathbf{F}_i - \eta\dot{\mathbf{r}}_i + \mathbf{R}_i + \mathbf{f}\delta_{i,N}$, where $m = 1$ is the mass of the bead, \mathbf{F}_i is the force acting on monomer i due to the presence of the nanotube and other polymer beads, \mathbf{R}_i is a random force related to the friction coefficient η by the fluctuation-dissipation theorem, and the last term represents the external (constant) stretching force acting along the radial direction of the nanotube on one of the end beads (see the Supplemental Material [28] for more details).

The mechanism of chain desorption is analyzed by monitoring the average number of beads detached from the nanotube. Because of the short-range nature of the surface interaction, the average fraction of beads detached from the nanotube $\phi_E(t)$ can be accurately determined from the interaction energy per monomer $E_{\text{wall}}(t)$ between the polymer and the surface of the nanotube as $\phi_E(t) = E_{\text{wall}}(t)/E_{\text{wall}}(0)$. The time evolution of the process of polymer desorption for different strengths of the pulling force f is shown in Fig. 2(a). During the desorption process, $|E_{\text{wall}}|$ decays with time, while the average desorption time for complete detachment τ increases with decreasing f . Figure 2(b) shows the dependence of the average fraction of beads adsorbed on the nanotube ϕ_E as a function of the reduced time $t/\tau(f)$, where $\tau(f)$ is the total desorption time for a given strength of the pulling force f . Within this representation, the data corresponding to different desorption conditions roughly collapse on a single curve.

Depending on the applied force, at long times, the chain is either completely adsorbed or completely detached from the surface of the nanotube. Figure 2(c) shows the desorption time τ as a function of the pulling force f for chains of different length. The polymer detaches if the force exceeds a critical value f_c , which is determined by the attractive surface potential and independent of the chain length and conformation. For given $f > f_c$, the desorption time τ increases with the size of the polymer chain; in addition, τ diverges as f approaches f_c according to a power law, $\tau \sim (f - f_c)^{-1}$. Figure 2(d) shows the behavior of τ as a function the chain length N for helical conformations with different pitch angles α [see the scheme in the inset of Fig. 2(d)]. For given α ($0 < \alpha \leq \pi/2$), τ follows a power law behavior $\tau \sim N^2$.

In addition, τ also depends dramatically on the helical pitch α . The detachment times for chains of the same length can differ by more than 1 order of magnitude, depending on the pitch angle.

This effect is further analyzed in Fig. 3. In the following, we express the initial number of beads per turn in a chain as

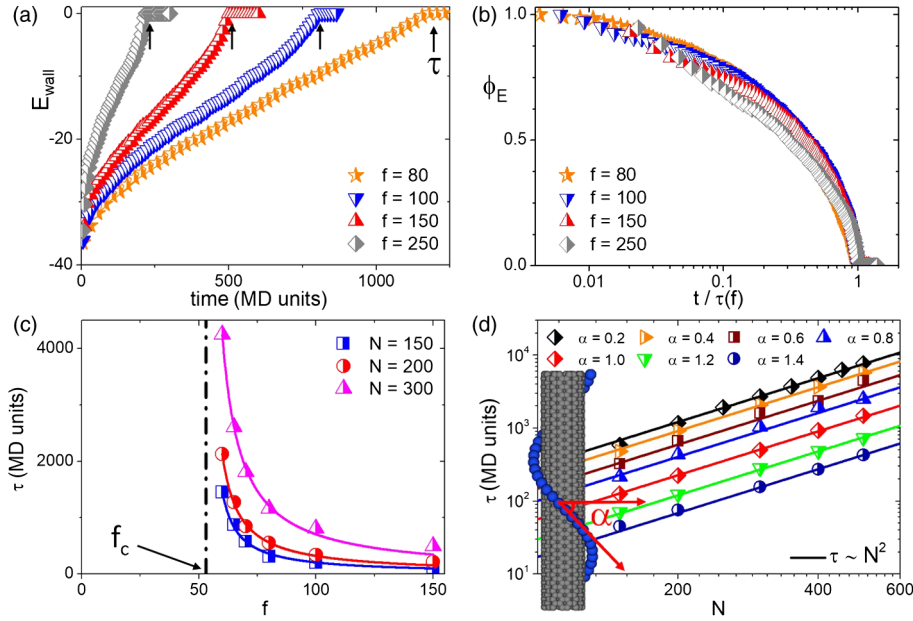


FIG. 2. Dynamics of force-assisted polymer desorption. (a) Average polymer or nanotube energy of interaction per monomer E_{wall} as a function of time ($N = 300$, $\alpha = 1.0$). The time where $E_{\text{wall}} = 0$ determines the characteristic time for complete desorption, τ ($N = 300$, $\alpha = 1.0$). (b) Fraction of desorbed beads ϕ_E as a function of the rescaled time $t/\tau(f)$. (c) Average desorption time τ vs applied force f , plotted for different chain lengths N . Here the lines shows that τ diverges at a critical force $f_c \sim 52$ as $\tau \sim (f - f_c)^{-1}$ (helix pitch $\sim 31.5b$ and ~ 37 monomers/turn). (d) τ vs chain size N for different helical conformations ($f = 150$). The lines show fits to $\tau \sim N^2$. Here α characterizes the pitch of the helical polymer conformation (see inset).

$n_0 \sim 2\pi R/b \cos(\alpha)$, where $R \sim 2.86 \pm 0.02$ is the average distance between the polymer beads and the center of the nanotube, and b the bond length. Thus, the initial number of windings is given by $n_w = N/n_0$. Figure 3(a) compares the time evolution of the fraction of desorbed monomers $\phi(t)$ for two systems with different number of windings n_w , but with the same chain size and pulling force. For the chain with the smaller number of windings around the tube ($n_w = 2.5$), complete desorption is reached after about 1400 MD time units. The desorption process slows down drastically for the system with $n_w = 14$, where only $\sim 20\%$ of the monomers are fully desorbed from the tube at the same time (i.e., 1400 MD time units). Figure 3(b) shows that, for a given N , τN^{-2} grows nearly exponentially with the number of windings.

The exponential dependence suggests that there might be a relation with the macroscopic phenomenon of belt friction, which occurs in situations where a rope is wrapped around a solid body. In that case, the equilibrium and dynamic properties depend on the rope configuration, the applied tension, and the angle θ between the rope and the cylinder along the surface of contact. In the simplest case of an inextensible rope wrapped around a cylindrical drum, the problem is described by the Euler-Eytelwein formula [29–31] (also known as the capstan equation): The applied tension F_0 decays exponentially with the friction coefficient between the rope and the surface μ and the total wrapping angle θ as $F(\theta) = F_0 \exp(-\mu\theta)$ [see the scheme

in Fig. 3(c)]. From rock climbing to belt machine design, this simple model has been widely used for more than 250 years. Figure 4(a) shows the behavior of the bond length stretching $\delta - \delta_0$ along the contour length of the polymer chain during the process of desorption. Here δ_0 is the average bond length for a chain lying on the tube in the absence of a pulling force. While in the fully desorbed portion of the polymer chain the bond stretching is nearly constant, in the adsorbed region $\delta - \delta_0$ decays rapidly along the polymer chain, in rough agreement with the capstan problem.

However, in contrast to macroscopic ropes, molecules in solution experience a substantial Stokes drag. To proceed, we will thus generalize the capstan equation to cases where the Stokes friction cannot be neglected. The tension at the n th chain bead is denoted $\gamma(n)$ (here $n = N$ corresponds to the free end, and $n = 0$ to the end where the force f is applied). It is constant [$\gamma = (f - f_c)$] for the desorbed chain part and depends on n for $n < N - m(t)$, where $m(t)$ is the number of adsorbed beads at time t . The force acting on one bead in the tangential direction due to the tension is thus $F_\gamma = \partial\gamma/\partial n$. In addition, in chain confined to a curved substrate, the tension generates a normal force $F_N = \gamma(2\pi/n_0)$ in the direction of the substrate. Because of this force, the bead experiences a solid friction force, which we approximate by Amontons's law, $F_\mu = \mu F_N$, with the kinetic friction coefficient μ . Finally, the Stokes friction force on the bead is given by $F_\zeta = \zeta v$, where ζ is the Stokes

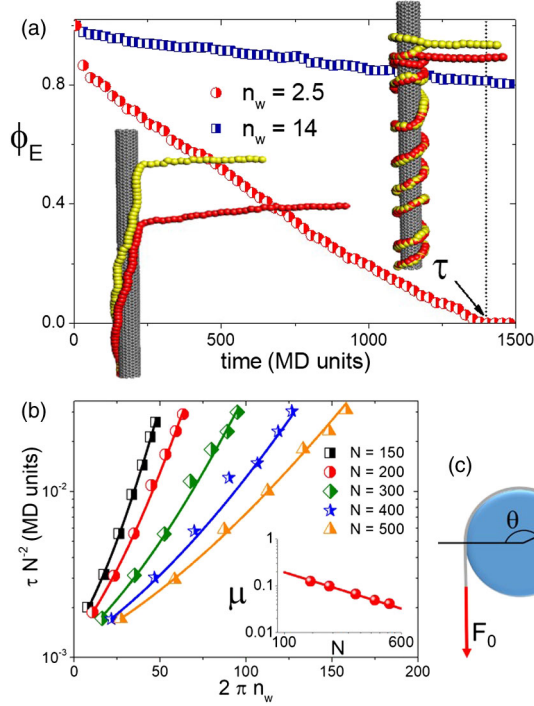


FIG. 3. Influence of the polymer conformation on the kinetics of polymer desorption. (a) Fraction of desorbed beads ϕ_E as a function of time. (Insets) Snapshots of the process of chain detachment at two times ($t = 25$ MD time steps, yellow beads; $t = 50$ MD time steps, red beads) for the two different polymer configurations. Note that the fraction of desorbed beads ϕ_E is strongly affected by the winding number n_w . Here $N = 300$ and $f = 60$. (b) When plotted against the wrapping angle between the polymer and the nanotube $2\pi n_w$, it is found that τN^{-2} grows as predicted by Eq. (1) ($f = 150$). The inset shows that the effective friction with the tube surface decreases with N as $\mu \sim 1/N$. (c) According to the capstan model, for an inextensible rope at equilibrium, $F(\theta) = \exp(\mu\theta)F_0$.

friction coefficient for a monomer moving on the surface of the tube, and $v = b|dm/dt|$ the average velocity of the chain. We consider an overdamped case where the velocity of the molecule results from a balance of forces; hence we require $F_\gamma + F_\mu + F_\zeta = 0$ for all beads with the boundary condition $\gamma(N) = 0$ at the free end of the molecule, and $\gamma[N - m(t)] = (f - f_c)$ at the detachment point. Combining everything (see the Supplemental Material [28]), the total desorption time can be expressed as

$$\tau_\mu = \tau_0 g(2\pi\mu n_w) \quad \text{with} \quad \tau_0 = \frac{\zeta b N^2}{2 f - f_c}, \quad (1)$$

where $g(x) = (2/x^2)(e^x - x - 1)$. Note that in the limit $\mu \rightarrow 0$, the scaling of the desorption time, $\tau_\mu \rightarrow \tau_0 \propto N^2/(f - f_c)$, agrees with the scaling observed for the desorption process from a flat substrate [32]. Figure 3(b) also shows the results of a fit of the numerical data with the model equation, Eq. (1). In spite of its simplicity, the model

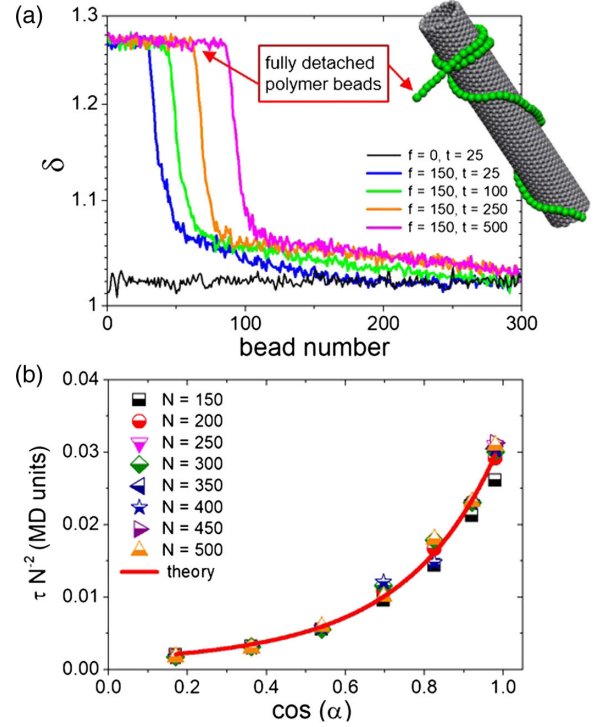


FIG. 4. Capstanlike dynamics of polymer desorption. (a) Average bond length deformation $\delta - \delta_0$ along the polymer chain at different simulation times ($\alpha = 0.6$, $N = 300$). As a reference, this panel also shows the behavior of δ in the absence of a pulling force. (b) τN^{-2} vs $\cos(\alpha)$ (symbols) and theoretical prediction (line) for the data shown in Fig. 3(b).

captures the behavior of τ vs n_w , and also the scaling observed in Figs. 2(c) and 2(d).

The inset of Fig. 3(b) shows that the fitted values for the kinetic friction coefficient μ depend on the chain length and seem to decay as $\mu \sim (\mu_0/N)$. Taking this result into account in a heuristic manner and using $n_w = Nb \cos(\alpha)/2\pi R$, we obtain $\tau N^{-2} \propto g[\mu_0 b \cos(\alpha)/R]$. Figure 4(b) shows that when τN^{-2} is plotted against $\cos(\alpha)$, all the data collapse onto a single curve with a functional form that is in excellent agreement with our model.

In summary, we have shown that the conformation of molecules adsorbed onto the surface of a carbon nanotube plays a crucial role in the dynamics of polymer detachment. In particular, wrapping molecules around the tubes can slow down the desorption dynamics by more than an order of magnitude. This effect might be important, e.g., for the kinetic stabilization of hybrid polymer-nanotube composites, where the interaction between different nanotubes is mediated by adsorbed polymers. The kinetic slowdown could also be exploited in applications such as DNA sequencing and SWCNT sorting.

The authors thank the Deutsche Forschungsgemeinschaft (Grants No. Schm 985/19 and No. SFB TRR 146), COST Action No. CA17139, supported by COST

(European Cooperation in Science and Technology [33]), the National Research Council of Argentina (CONICET), and Universidad Nacional del Sur (UNS) for the financial support.

*dvega@uns.edu.ar

[†]Also at Institute for Physical Chemistry, Bulgarian Academy of Sciences, 1113 Sofia, Bulgaria.

- [1] J. C. Turner and P. van de Griend, *History and Science of Knots* (World Scientific, Singapore, 1996).
- [2] S. J. Gerbode, J. R. Puzey, A. G. McCormick, and L. Mahadevan, *Science* **337**, 1087 (2012).
- [3] A. R. Studart and R. M. Erb, *Soft Matter* **10**, 1284 (2014).
- [4] J. Fleagle and J. G. Fleagle, *Primate Adaptation and Evolution*, 3rd ed. (Academic Press, New York, 2013).
- [5] H. Fu, S. Xu, and Y. Li, *Sci. Rep.* **6**, 30310 (2016).
- [6] M. Zheng, A. Jagota, M. S. Strano, A. P. Santos, P. Barone, S. G. Chou, B. A. Diner, M. S. Dresselhaus, R. S. Mclean, G. B. Onoa, G. G. Samsonidze, E. D. Semke, M. Usrey, and D. J. Walls, *Science* **302**, 1545 (2003).
- [7] M. Zheng, A. Jagota, E. D. Semke, B. A. Diner, S. R. L. Mclean, R. E. Richardson, and N. G. Tassi, *Nat. Mater.* **2**, 338 (2003).
- [8] A. Karatrantos and N. Clarke, *Soft Matter* **7**, 7334 (2011).
- [9] A. Karatrantos, R. J. Composto, K. I. Winey, M. Kröger, and N. Clarke, *Macromolecules* **45**, 7274 (2012).
- [10] G. Allegra, G. Raos, and M. Vacatello, *Prog. Polym. Sci.* **33**, 683 (2008).
- [11] L. Meng, X. Zhang, Q. Lu, Z. Fei, and P. J. Dyson, *Biomaterials* **33**, 1689 (2012).
- [12] H. Meng, K. Andresen, and J. V. Noort, *Nucleic Acids Res.* **43**, 3578 (2015).
- [13] S. Prakash, M. Malhotra, W. Shao, C. Tomaro-Duchesneau, and S. Abbasi, *Adv. Drug Delivery Rev.* **63**, 1340 (2011).
- [14] D. A. Heller, H. Jin, B. M. Martinez, D. Patel, B. M. Miller, T. K. Yeung, P. V. Jena, C. Höbartner, T. Ha, S. K. Silverman, and M. S. Strano, *Nat. Nanotechnol.* **4**, 114 (2009).
- [15] N. Yang and X. Jiang, *Carbon* **115**, 293 (2017).
- [16] X. Tu, S. Manohar, A. Jagota, and M. Zheng, *Nature (London)* **460**, 250 (2009).
- [17] H. Wang, G. I. Koleilat, P. Liu, G. Jiménez-Osés, Y. C. Lai, M. Vosgueritchian, Y. Fang, S. Park, K. N. Houk, and Z. Bao, *ACS Nano* **8**, 2609 (2014).
- [18] D. Roxbury, A. Jagota, and J. Mittal, *J. Phys. Chem. B* **117**, 132 (2013).
- [19] D. Roxbury, J. Mittal, and A. Jagota, *Nano Lett.* **12**, 1464 (2012).
- [20] D. Roxbury, A. Jagota, and J. Mittal, *J. Am. Chem. Soc.* **133**, 13545 (2011).
- [21] I. M. Kulić, H. Mohrbach, V. Lobaskin, R. Thakkar, and H. Schiessel, *Phys. Rev. E* **72**, 041905 (2005).
- [22] D. Roxbury, X. Tu, M. Zheng, and A. Jagota, *Langmuir* **27**, 8282 (2011).
- [23] Y. Liu, C. Chipot, X. Shao, and W. Cai, *J. Phys. Chem. C* **115**, 1851 (2011).
- [24] C. D. Von Bargen, C. M. MacDermaid, O.-S. Lee, P. Deria, M. J. Therien, and J. G. Saven, *J. Phys. Chem. B* **117**, 12953 (2013).
- [25] X. Zhao, Y. Liu, S. Inoue, T. Suzuki, R. O. Jones, and Y. Ando, *Phys. Rev. Lett.* **92**, 125502 (2004).
- [26] A. Ghosh, D. I. Dimitrov, V. G. Rostiashvili, A. Milchev, and T. A. Vilgis, *J. Chem. Phys.* **132**, 204902 (2010).
- [27] G. S. Grest and K. Kremer, *Phys. Rev. A* **33**, 3628 (1986).
- [28] See Supplemental Material at <http://link.aps.org/supplemental/10.1103/PhysRevLett.122.218003> for additional results on the desorption dynamics and desorption times including an error analysis and for a more detailed derivation of the Generalized Capstan Equation.
- [29] L. Euler, *Methodus Inveniendi Lineas Curvas Maximi Minimive Proprietate Gaudentes, Sive Solutio Problematis Isoperimetrici Latissimo Sensu Accepti, Additamentum I (De Curvis Elasticis)* (apud Marcum-Michaelem Bousquet & Socios, Lausanne, Geneva, 1744), pp. 245–320.
- [30] L. Euler, *Mem. Acad. Sci. Berlin* **18**, 265 (1769).
- [31] J. A. Eytelwein, *Handbuch der Statik fester Körper, Mit vorzüglicher Rücksicht auf ihre Anwendung in der Architektur*, Vol. 2 (Realschule Berlin, Berlin, 1808), pp. 245–320.
- [32] J. Paturej, A. Milchev, V. G. Rostiashvili, and T. A. Vilgis, *Macromolecules* **45**, 4371 (2012).
- [33] See <http://www.cost.eu>.